In-orbit Response versus Scan-angle (RVS) Validation for the GOES-16 ABI Solar Reflective Bands

Fangfang Yu[1], Xi Shao[1], Xiangqian Wu[2], and Haifeng Qian[1]

1: ERT, Inc., Laurel, MD 20707; 2: NOAA/NESDIS/STAR, College Park, MD 20740

Abstract

The weather instrument of Advanced Baseline Imager (ABI) is the mission critical instrument on-board the GOES-16 satellite. Compared to the predecessor GOES Imager, GOES-16 ABI has many new advanced technical devices and algorithms to improve the data quality, including the double scan-mirror system. To validate the in-orbit response versus scan-angle (RVS), the Moon is used as a reference target for this purpose. During the post-launch test (PLT) and post-launch product test (PLPT) period, a series of special scans were conducted to chase and collect the lunar images at optimal phase angle range when it transited across the space within the ABI Field of Regard (FOR) from West to East. Analyses of the chasing events above and below the Earth indicated that the RVS variations at the East-West (EW) direction are generally less than 1% for all the six solar reflective bands. Same method is being applied to validate the GOES-17 ABI spatial uniformity for the visible and near-infrared (VNIR) bands.

Keyword: GOES-16 ABI, VNIR bands, Response versus Scan-angle (RVS), spatial uniformity, solar reflective bands, and PLT/PLPT.

1. INTRODUCTION

The weather instrument of Advanced Baseline Imager (ABI) is the primary payload onboard the NOAA Geostationary Environmental Operational Satellite (GOES)-16 which was launched on 19 November 2016 and became operational as GOES-East since after 18 December 2017. Compared to its predecessor GOES Imager, ABI is faster and more powerful with increased spatial, spectral, and temporal resolutions. These advanced features are based on a completely new data collection mechanism in the form of two orthogonal scan mirrors which scan the ABI's field of regard (FOR) in the North-South (NS) and East-West (EW) directions independently and simultaneously. As the coating materials of the scan mirrors have absorptive feature, the energy received by the detectors should be corrected with the incident angles of the incoming light [1].

The angular reflectance and emissivity correction parameters were carefully measured on the ground for each ABI band. Along with the other prelaunch measured instrument parameters, the mirror coefficients were implemented operationally to generate the early Level1B (L1B) data. A set of special scan testing were designed and executed during the post-launch testing (PLT) and post-launch product testing (PLPT) period to validate the instrument performance. For the infrared (IR) bands, it was found in the early PLT/PLPT period that the prelaunch mirror emissivity parameters caused IR calibration anomalies of diurnal calibration variation and the periodic inferred calibration anomaly (PICA) and must be updated using the in-orbit measurements. The updated mirror coefficients, which were derived based on the measurement of the thermal uniform space region around the Earth, significantly improve the data quality [2].

Similarly, a stable reflective reference is needed to validate the spatial uniformity of ABI visible and near-infrared (VNIR) bands across the ABI FOR. The Moon, due to its exceptionally stable reflectance and negligible atmospheric effects, is used as a stable reference in this study to validate the response versus scan-angle (RVS) for the ABI solar reflective bands. As the lunar surface is not uniform, an accurate photometric model is needed to characterize the directional reflectance of the illuminated surface at varying phase angle and libration conditions. The United States Geological Survey (USGS) deployed a dedicated ground-based facility, the Robotic Lunar Observatory (ROLO) with 32

Earth Observing Systems XXIII, edited by James J. Butler, Xiaoxiong (Jack) Xiong, Xingfa Gu, Proc. of SPIE Vol. 10764, 107640E · © 2018 SPIE · CCC code: 0277-786X/18/$18 · doi: 10.1117/12.2322154

solar reflective bands ranging from 350 to 2450 nm, for the radiometric observation of the Moon over 8 years. Based on the thousands of multiple spectral lunar images obtained from the ROLO observatory, the USGS photometric lunar model, also called the ROLO model, was developed to predict the spectral irradiance of gibbous Moon [3]. The relative accuracy of the ROLO model can be less than 1% within certain phase angle range [4]. EUMETSAT recently implemented the ROLO model and make it available to within the Global Satellite Inter-Calibration System (GSICS). In this study, the GSICS Implementation of the ROLO model (GIRO) is used to estimate the lunar irradiance for ABI.

2. ABI INSTRUMENT ANG GROUND SEGMENT DATA PROCESSING

Built by Harris, ABI has six visible and near infrared (VNIR) bands and 10 infrared bands imaging the environment of the Western Hemisphere for weather forecasting, disaster monitoring and climate studies. The detectors of the 16 bands are deployed at three focal plane models (FPM): VNIR 0.47µm to 2.25µm, mid-wave IR (MWIR) from 3.9µm to 8.5µm and longwave IR (LWIR) from 9.6µm to 13.3µm [5]. Detectors of wavelength less than 1µm are made of Silicon, while all the others are made of Mercury-Cadmium-Telluride (HgCdTe). The detector array of each band consists of three or six detector columns of detectors for redundancy. Each column has hundreds to thousands of row of detectors, depending on the wavelength (Table 1). While in operation, only one column detector from each row is selected based on the detector performance testing results conducted on the ground and in-orbit. The selected detector is called best detector selection (BDS).

Figure 1 illuminates the ABI optical system: the incident radiation passes through the two scan mirror system, four-mirror anastigmat telescope, and then split into the three FPMs for imaging. The two scan mirror system consists of the North-South (NS) and the East-West (EW) scan mirrors. These two mirror can be operated individually and simultaneously for a variety of combined scan patterns and pointing to any position within the FOR. Also, polarization caused by the NS scan mirror can be cancelled by the EW scan mirror around nadir area [5].

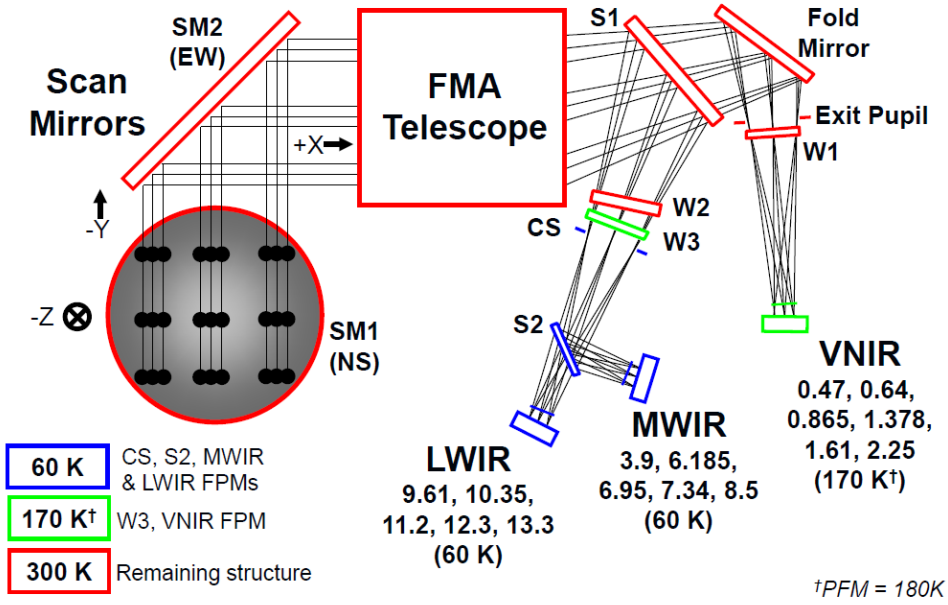

Figure 1. Conceptual ABI optical architecture [5]. SM1 and SM2 are the two scan mirrors for the north-south and east-west directions, respectively. VNIR, MWIR and LWIR are the three FPMs.

Unlike GOES Imager which scans the Earth in a boustrophedonic manner with one scan mirror, ABI scans swaths from west to earth and steps from north to south across the Earth FOR with the two scan mirrors [6]. During the

operation, GOES-16 ABI is mainly operated with the Mode 3. This 15-minute timeline consists of 22 swaths of Full-Disk (FD) of the Earth, three sets of 6 swaths of Continental United States (CONUS), and 30 sets of 2 swaths of Mesoscale (MESO) regions. While the FD and CONUS scans have fixed locations, the MESO scans can be pointed to any position within the ABI FOR due to the agile two-scan-mirror system [7]. The lunar images are collected using the MESO scans when it appears in the space within the ABI FOR.

To provide high quality of radiance data, ABI has in-orbit calibration devices for all the 16 bands: the Spectralon Solar Diffuser (SD) as the solar calibration target (SCT) for the VNIR bands and the temperature controlled blackbody as the internal calibration target (ICT) for the IR bands. The two-point method is used for the radiometric calibration. The radiometric calibration equation for the VNIR bands is shown with Equation (1) [8]. The on-board solar diffuser (SD) is used as the bright reference and the deep space as the dark reference. Detector non-linear response is corrected with a quadratic function. While the quadratic term (q) for each detector is fixed, the linear calibration coefficient (m) is updated after every solar calibration event.

$$R_{target} = \frac{m\Delta C_{target} + q\Delta C_{target}^2}{\rho_{EW}^{target}\rho_{NS}^{target}} \quad (1)$$

where R_{target} is the radiance of scanned target; m is the calibration coefficient determined in-orbit; q is the quadratic term, fixed; ΔC_{target} is the target count offset to the space; $\rho_{NS}^{target} and\ \rho_{EW}^{target}$ are the reflectance of the NS and EW scan mirror at the incident angle of the scanned target, respectively.

The GOES-R Ground Segment (GS) receives, processes and disseminates the ABI data. The L0 data downlinked from the satellite is uncompressed and converted to L1A data which are the satellite measurements in count. The measured count (L1A data) is then radiometrically calibrated using the on-orbit target measurements (L1α or L1alpha), navigated with Global Position System (GPS) and Kalman filter techniques (L1β or L1beta), and finally rectified into the fixed grid of a GR80 ellipoid viewed from the idealized geostationary position with kernel-based resampling algorithm (L1B) [7]. The image grid in L1alpha and L1beta is referred as "sample", and the fixed grid in L1B images is as "pixel". The lunar images are processed into L1alpha format which is radiometrically calibrated but not navigated. The nominal sample size in angular sample distance (ASD) is shown in Table 1.

Table 1. Spectral wavelength, nominal sample ASD at EW and NS directions, detector material, detector columns and rows for ABI bands [5].

ABI Band	Central wavelength (μm)	ASD EW (μrad)	ASD NS (μrad)	Columns	Rows
1	0.47	22	22.9	3	676
2	0.64	11	10.5	3	1460
3	0.87	22	22.9	3	676
4	1.38	44	42	6	372
5	1.61	22	22.9	6	676
6	2.25	44	42	6	372
7	3.9	44	47.7	6	332
8	6.2	44	47.7	6	332
9	6.9	44	47.7	6	332
10	7.3	44	47.7	6	332
11	8.5	44	47.7	6	332
12	9.6	44	47.7	6	332
13	10.4	44	38.1	6	408
14	11.2	44	38.1	6	408
15	12.3	44	38.1	6	408
16	13.3	44	38.1	6	408

3. ABI LUNAR IMAGE COLLECTIONS AND DATA REPROCESSING

The lunar images are collected when the Moon moves from West to East in the space within the ABI FOR. As previously mentioned, the Mode 3 MESO scans are used to collect the lunar images. When the Moon transits across the space above or below the Earth Pole, it covers a large part of ABI scan earth range at the EW direction (Figure 2). Thus these lunar images beyond Earth Polar regions are unique to validate the EW spatial uniformity. During the GOES-16 post-launch test (PLT) and post-launch product test (PLPT) period, as requested by the GOES-R Calibration Working Group (CWG), the Moon was consecutively scanned using all the MESO scans within its transit periods of 02/11/2017 and 04/12/2017. This kind of consecutive moon image collection event is called as moon-chasing. Each ABI MESO scan consists of two swaths scanning adjacently at NS direction. As the ABI VNIR focal plane model is about 0.9^o in height which is larger than about 0.52^o of Moon diameter as viewed from the geostationary orbit, the Moon is thus scanned using one of the two swaths.

Figure 2. ABI FOR (in dash circle) and the Earth. The lunar images can be collected when the Moon appears within the annular space.

However, the Ground Segment was not stable before GOES-16 ABI became operational. A missing line can be observed in all the B06 images collected on 02/11/2017. Also, all the VNIR data experienced abnormal radiometric calibration between 03/16/2017 and 04/29/2017. To overcome these issues, an offline science package was developed to reprocess these lunar L1alpha data from L1A data. The L1A data were ingested with the GOES-R ABI Trending and Data Analysis Toolkit (GRATDAT). The L1A was validated to ensure the correct values used for the further analysis. The detector solar calibration coefficients on 02/11/2017 derived by the CWG team were used for the data re-processing.

4. LUNAR IRRADIANCE CALCULATION

The ratio between the measured and the modelled irradiance is used to characterize the RVS variations for the six ABI VNIR bands [9]. Investigation of the ABI scan data showed that ABI scan rate is very stable and consistent. No apparent Earth shine straylight and band-to-band cross-talk impacts can be observed from the lunar MESO scan images as well as the lunar north-south scan data [10]. Very slight ghost straylight impact can be observed at the B06 images at the north edge of the lunar swath near the moon [10]. For the convenient data processing, the lunar image is then subset to the size of 400x372 for B01, B03 and B05, 800x676 for B04 and B06, and 1600x1460 for B02. The lunar irradiance for a given band (I) is thus measured as follows:

$$I_{ABI} = \frac{\Omega}{f_{oversampling}} \sum_i^{row} \sum_j^{col} R_{i,j} \qquad (2)$$

Where Ω is the sample solid angle, $f_{oversampling}$ is the oversampling factor and $R_{i,j}$ is the radiance for the sample in row i and column j in the subset images ABI has fixed sample solid angle (Ω). The oversampling factor is also a constant value as the ABI scan rate and the sample integration time and rate are all constant. Therefore, the variables of sample solid angle and the oversampling factor can be cancelled out when the irradiance ratio (Equation 3) is normalized with the mean value ($\overline{Ratio}$) (in Equation 4).

$$Ratio = \frac{I_{ABI}}{I_{ROLO}} \qquad (3)$$

$$Norm_{Ratio} = \frac{Ratio}{\overline{Ratio}} \qquad (4)$$

5. RESULTS AND DISCUSSIONS

Figure 3 is an example of the subset lunar images for the six bands collected on 02/11/2017. As the BDS detectors are not selected from the same column, some small pikes can be seen from the edges of the illuminated moon. This is especially the case for B04 which has BDS from all the six columns. The moon looks wiggled in the B04 image. We can shift the BDS detectors with the relative detector position (RDP) map to achieve the smooth lunar edge. This function is used to validate the correct implementation of the BDS map in the PLT/PLPT period.

Figure 3. GOES-16 ABI lunar images. Note that spatial resolution is about 1/16 of those of B04 and B06 for B2, and the ¼ for B01, B03 and B05, shown in Table 1.

The Moon moved across the space above the North Pole on 02/11/ 2017 and below the South Pole on 04/12/2017 (Figure 4). On 02/12/2017, the Moon was successfully chased and collected as requested during the whole event. As

shown in the Figure, it can be scanned before and after it entered and left the FOR, respectively. This is because that while the light of sight (LOS) of ABI was pointing to an area near the edge of the FOR, the MESO swath can scan outside the FOR and thus part of the swath frames are thus beyond the FOR . For B02, the EW scan angle ranged between about -6° to +6°. The scan angle range differed slightly among the different VNIR band due to their different detector deployment positions in the PFM.

Several issues occurred for the lunar chasing event conducted on 04/12/2017. First, the MESO didn't start to chase the Moon about 10 minutes later after it entered into the FOR. Secondly, the MESO scans stopped collecting the Moon data for about 15 minutes within the chasing period. During this period, the MESOs were commanded to scan the Earth instead of the Moon. The red spike in right of Figure 4 indicated this 15-minute anomaly. For these reason, the valid scan angle range was discontinuous and relatively narrow for the event conducted on 04/12/2017.

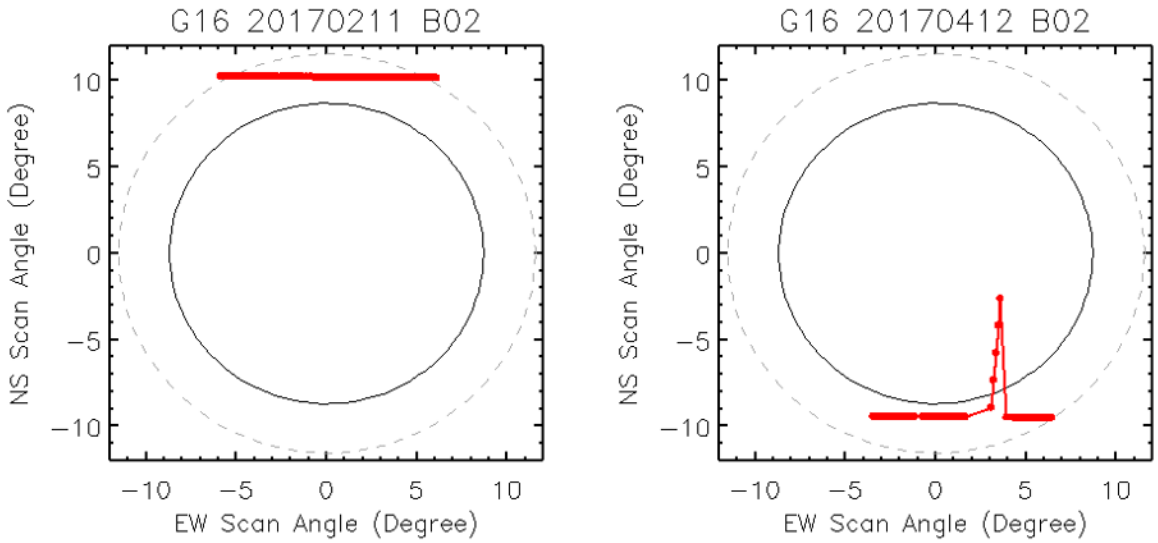

Figure 4. Scan angle distribution of the Moon (red line) within the ABI FOR for the lunar chasing data collected on 02/11/2017 (left) and 04/12/2017 (right). The solid circle is the Earth and the dash gray one is the FOR.

Figure 5 and Figure 6 are the time-series of the normalized irradiance ratio for the data collected on 02/11/2107 and 04/12/2017, respectively. The variation of the lunar irradiance ratio, which can be considered as RVS variation, is generally within 1% for all the 6 bands in these two days. B01 seems to have a persistent certain structure within the 15-minute timeline in both two day data. Further investigation on the root cause to the structure is needed.

The trending on 04/12/2017 in general agrees well with those on 02/11/2017 for each band. This may suggest the trending observed on 02/11/2017 in Figure 5 should be mainly attributed to the residual of spatial uniformity correction at the EW direction. Same method is now being applied to GOES-17 ABI. Comparison of the RVS variations from GOES-16 and GOES-17 can help to distinguish the performance of instruments and the lunar irradiance model with more confidence.

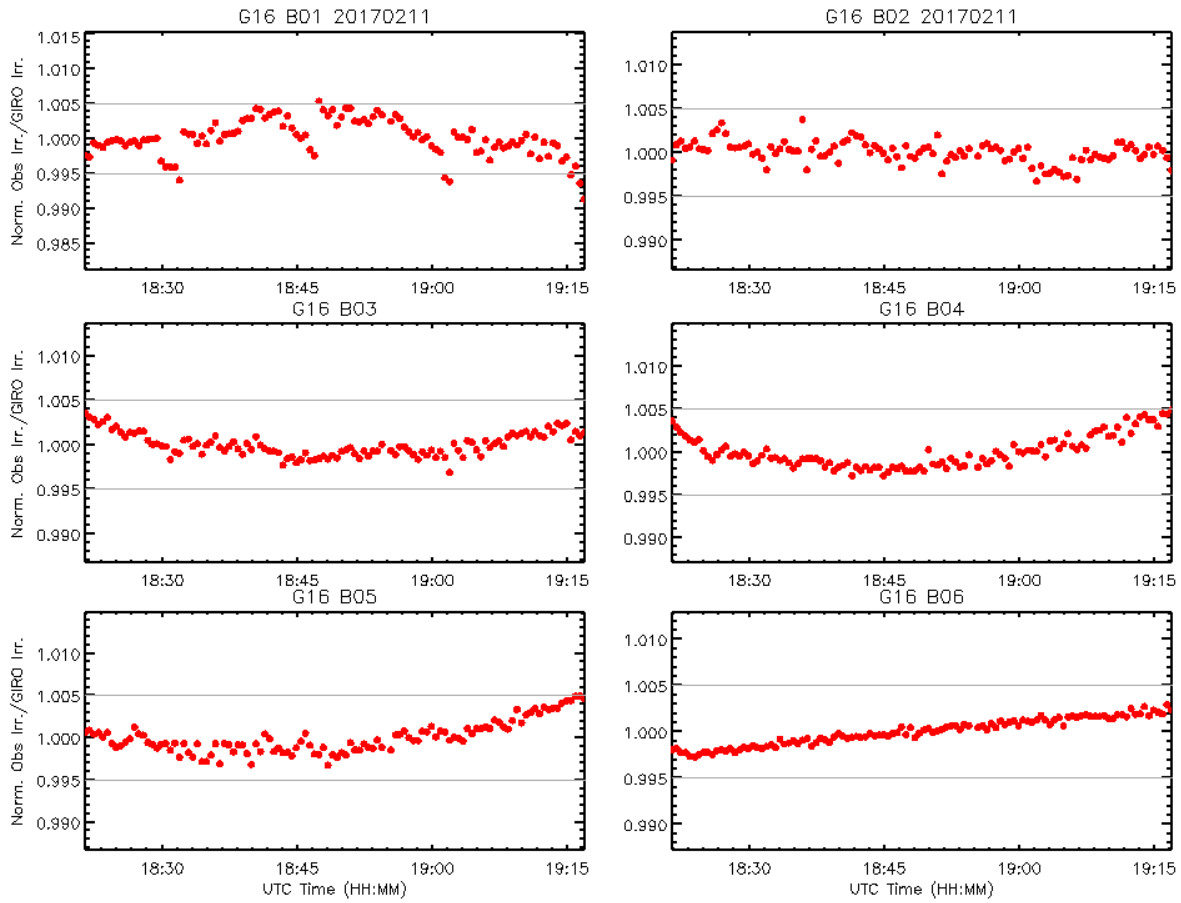

Figure 5. Time-series of the normalized lunar irradiance ratio for the six VNIR bands collected on 02/11/2017.

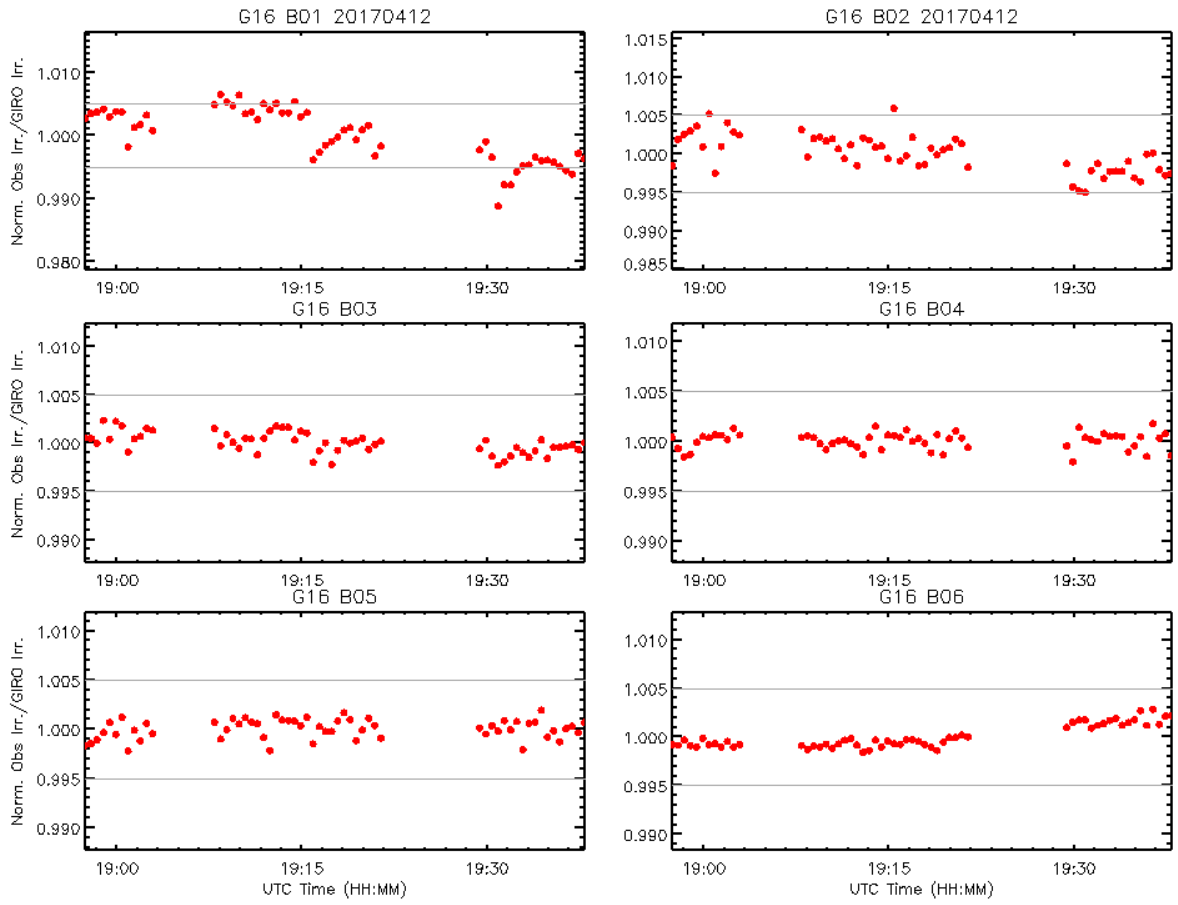

Figure 6. Same as Figure 5, but for data collected on 04/12/2017.

6. SUMMARY

Two lunar chasing events collected on 02/11/2017 and 04/12/2017 were used to validate the GOES-16 ABI RVS at the EW direction. Results of these two chasing events in general agree with each other. The RVS variations are in general within 1% for the all six GOES-16 VNIR bands. Yet certain consistent structure can be observed at B01 data, which needs further investigation. Same method is currently being applied to GOES-17 ABI during the PLT/PLPT period. Results from GOES-16 and GOES-17 data can help to distinguish the performance of the GIRO model and ABI instruments.

Acknowledgement:
This work is funded by GOES-R program. We would like to thank GOES-R PRO, Flight and MOST teams for the help to collect the special scan data and EUMETSAT for sharing the GIRO model within the GSICS community. We would also like to thank Dr. Hyelim Yoo in helping downloading the L0 data.

REFERENCE

1. Weinreb, M., Jamieson, M., Fulton, N., Chen, Y., Johnson J., Bremer, J., Smith, C., and Baucom J., "Operational calibration of Geostationary Operational Environmental Satellite-8 and -9 images and sounders," *Applied Optics*, 36(27), 6895-6904 (1997).

2. Yu, F. et al. “Validations of GOES-16 ABI Infrared Spatial Response Uniformity”, *SPIE Proc*, San Diego, CA (2018).
3. H. Kieffer and T. Stone, “The spectral irradiance of the Moon,” Astron. J., **129**, 2887-2901 (2005).
4. Meygret, A. Blanchet, G., Colzy S., Gross-Colzy, L. “Improving ROLO lunar albedo model using PLEIADES-HR satellites extra-terrestrial observations,” *SPIE Optical Engineering and Applications, Earth Observing Systems XXII,* San Diego, August (2017).
5. Griffith, P. “ABI’s unique calibration and validation capabilities,” *EUMETSAT Meteorological Satellite Conference*, Toulouse, France, (2015).
6. Kalluri, S. Alcala, C. Carr, J., Griffith, P., Lebair, W., Lindsey, D. Race, R. Wu, X., and Zierk, S., “From photons to pixels: processing data from the Advanced Baseline Imager,” *Remote Sensing*, 10(177), doi:10.3390/rs10020177 (2018).
7. Carlomusto, M., “GOES-R Series product definition and users’ guide (PUG),” Vol. 3, Level 1B Products, 2017.
8. Dalta, R., Shao, X., Cao, C. and Wu, X., “Comparison of the calibration algorithms and SI traceability of MODIS, VIIRS, GOES, and GOES-R ABI Sensors,” *Remote Sensing*, 8(126), doi:10.3390/rs8020126 (2016).
9. Wu, X., Stone, T., Yu. F, and Han, D., “Vicarious calibration of GOES Imager visible channel using the Moon,” Proc. SPIE, **6296**, 62960Z, doi:10.1117/12.681591 (2006).
10. Yu, F., Shao, X., Wu, X. and Qian, H., “Applications of GOES-16 ABI lunar north-south scans (NSS): detector out-of-field, blooming and uniformity responses,” *CALCON meeting*, Logan UT, June 2018.